

An Operational Definition of Topological Order

Amit Jamadagni* and Hendrik Weimer

Institut für Theoretische Physik, Leibniz Universität Hannover, Appelstraße 2, 30167 Hannover, Germany

The unrivaled robustness of topologically ordered states of matter against perturbations has immediate applications in quantum computing [1] and quantum metrology [2], yet their very existence poses a challenge to our understanding of phase transitions. In particular, topological phase transitions cannot be characterized in terms of local order parameters, as it is the case with conventional symmetry-breaking phase transitions. Currently, topological order is mostly discussed in the context of nonlocal topological invariants [3, 4] or indirect signatures like the topological entanglement entropy [5–7]. However, a comprehensive understanding of what actually constitutes topological order is still lacking. Here we show that one can interpret topological order as the ability of a system to perform topological error correction. We find that this operational approach corresponding to a measurable observable does not only lay the conceptual foundations for previous classifications of topological order, but it can also be applied to hitherto inaccessible problems, such as the question of topological order for mixed quantum states arising in open quantum systems. We demonstrate the existence of topological order in open systems and their phase transitions to topologically trivial states, including topological criticality. Our results demonstrate the viability of topological order in nonequilibrium quantum systems and thus substantially broaden the scope of possible technological applications. We therefore expect our work to be a starting point for many future theoretical and experimental investigations, such as the application of our approach to fracton [8, 9] or Floquet [10, 11] topological order, or the direct experimental realization of the error correction protocol presented in our work for the development of future quantum technological devices.

Topologically ordered phases are states of matter that fall outside of Landau’s spontaneous symmetry breaking paradigm and can essentially be classified into symmetry-protected topological order or intrinsic topological order [12]. For the former, the existence of a symmetry is required to maintain topological order, i.e., when the symmetry is broken the system immediately returns to a topologically trivial state. In some cases, topological order can be captured in terms of topological invariants such as the Chern number [4], but being based on single-particle wave functions, their extension to inter-

acting systems is inherently difficult [13]. Alternatively, topological order has been discussed in terms of nonlocal order parameters often related to string order [14–17], but the main difficulty of this approach is that such string order can also be observed in topologically trivial phases [18]. From a conceptual point of view, a particularly attractive definition of topological order is the impossibility to create a certain quantum state from a product state by a quantum circuit of finite depth [19]. However, since this is equivalent to the uncomputable quantum Kolmogorov complexity [20], it has very little practical applications. Hence, most analyses of topological ordered systems have been centered around indirect signatures such as the topological entanglement entropy [5–7] or minimally entangled states [21, 22], but even those quantities can prove difficult to interpret [23, 24].

Here, we overcome the limitations of the previous approaches to topological order by understanding topological order as the intrinsic ability of a system to perform topological error correction, giving rise to an operational definition of topological order that can be readily computed. To make this definition mathematically precise, we call a system to be in a topologically ordered state if it can be successfully corrected by an error correction circuit of finite depth. One key advantage of our approach is that the error correction circuit does not have to be optimal, as it only requires to reproduce the correct finite size scaling properties, which can be expected to be universal across a topological phase transition. This puts our approach in stark contrast with the classification of topological error correction codes in terms of their threshold values [25], as the latter is a nonuniversal quantity. Symmetry protected topological order can be represented within our error correction formalism by imposing certain symmetry constraints on the error correction circuit. Compared to previous approaches to topological order, another striking advantage of our error correction method is that it corresponds to an actual observable, which can be measured in an experiment.

To demonstrate the viability of our error correction approach in a concrete setting, we turn to the toric code model, which serves as a paradigm for intrinsic topological order [1]. Its Hamiltonian is given by a sum over two classes of spin 1/2 operators describing four-body interactions, A_v and B_p , acting on vertices v and plaquettes p , respectively, according to

$$H_{TC} = -E_0 \left(\sum_v \underbrace{\sigma_\alpha^x \sigma_\beta^x \sigma_\gamma^x \sigma_\delta^x}_{A_v} + \sum_p \underbrace{\sigma_\mu^z \sigma_\nu^z \sigma_\rho^z \sigma_\sigma^z}_{B_p} \right), \quad (1)$$

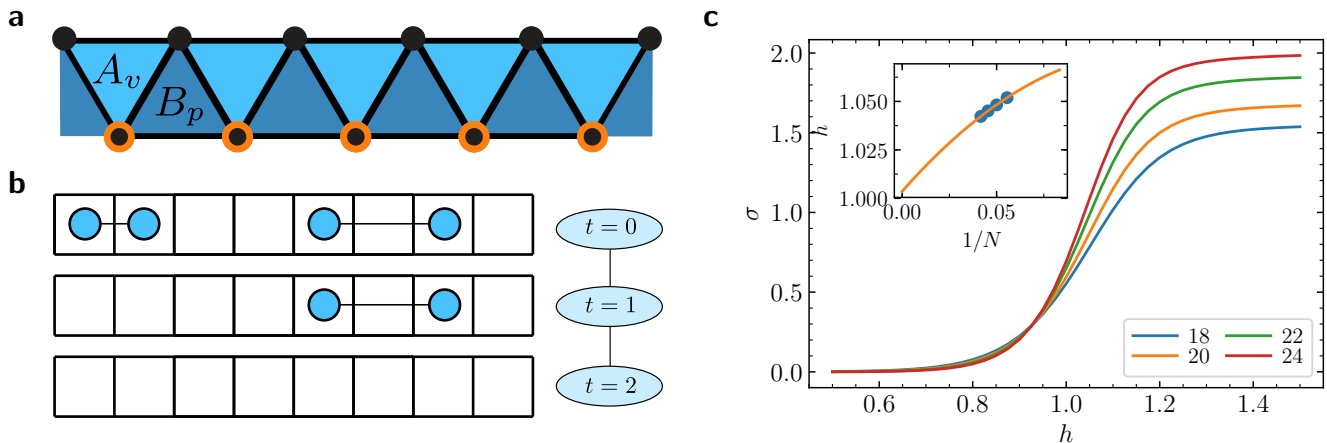


FIG. 1. Topological order in a quasi-1D toric code model. (a) The A_v and B_p operators are arranged along two rails of sites such that the perturbation on the lower rail (orange) maps onto the 1D transverse field Ising model. (b) Example of the error correction procedure for $N = 8$ Ising spins containing four errors, with the state of the system shown after t timesteps of the algorithm. The errors are fused along the horizontal strings, with the total error correction depth being $t_d = 2$. (c) Standard deviation n_σ of the circuit depth for different system sizes. Above the topological transition, the circuit depth diverges in the thermodynamic limit, with a finite size scaling analysis (inset) including terms up to N^{-2} yielding $h_c = 1.004(5)$.

where $\sigma_i^{x,z}$ denotes the Pauli matrix acting on site i . The robustness of topological order of the ground state can be analyzed with respect to the response of a perturbation describing a magnetic field, i.e., $H = H_{TC} - h \sum_i \sigma_i^x$. Importantly, the perturbed toric code can be mapped onto an Ising model in a transverse field using a highly non-local unitary transformation [26]. The phase transition from the topologically ordered to the trivial state then corresponds to the phase transition between the paramagnet and the ferromagnet in the Ising model [27]. Here, we will be interested in the case where the perturbed toric code can be mapped exactly onto the one-dimensional (1D) Ising model, which can be realized by imposing the right boundary condition [24], see Fig. 1. Our approach has the advantage that the critical point of the topological phase transitions is known to be exactly at $h_c = 1$. Note that the quasi-1D nature of the toric code model results in the four-body interactions in Eq. (1) being replaced by three-body interactions.

For the topological order arising in the toric code, the required topological error correction can be readily expressed in terms of the Ising variables $S_v = A_v$ and $S_p = B_p$, where each spin having $S_i^z = -1$ corresponds to the presence of an error. As a first step of the error correction algorithm, a syndrome measurement is performed, i.e., all the Ising spins are measured in their S^z basis, corresponding to the measurement of both the A_v and B_p degrees of freedom in the original toric code model. Under the perturbation, the observables S_i^z exhibit quantum fluctuations, therefore it is necessary to perform a statistical interpretation of the depth of the error correction circuit. Here, we find that the standard deviation of the circuit depth exhibits substantially better finite size scaling behavior than the mean, hence we use the

former for the detection of topological order in the following. The error correction circuit is then implemented in a massively parallel way by decorating each of the detected errors by a walker that travels through the system until it encounters another error, upon which the two errors are fused and removed from the system [28], see the Methods section for details. Figure 1 demonstrates that our error correction approach is indeed able to detect the topological phase transition, including the identification of the correct critical point at $h_c = 1$.

Let us now extend our approach to mixed quantum states, where previous works have shed some light on topological properties [29–33], but a universally applicable definition of topological order has remained elusive so far. This extension is straightforward, as the implementation of the topological error correction channel can be applied to mixed states as well. Here, we consider mixed states arising in open quantum systems with purely dissipative dynamics given in terms of jump operators c_i according to the Markovian quantum master equation $d\rho/dt = \sum_i c_i \rho c_i^\dagger - \{c_i^\dagger c_i, \rho\}/2$. Dissipative variants of the toric code can be constructed by considering the jump operators

$$\begin{aligned} c_i^v &= \sqrt{\gamma_v} \sigma_i^z (1 - A_v)/2, i \in v \\ c_i^p &= \sqrt{\gamma_p} \sigma_j^x (1 - B_p)/2, j \in p \end{aligned}$$

with rates $\gamma_{v,p}$, which result in the toric code ground states being steady states of the quantum master equation [34]. As before, we now consider the robustness of topological order to an additional perturbation. Here, we will first consider again a quasi one-dimensional model analogous to Fig. 1a, in which the perturbation is given

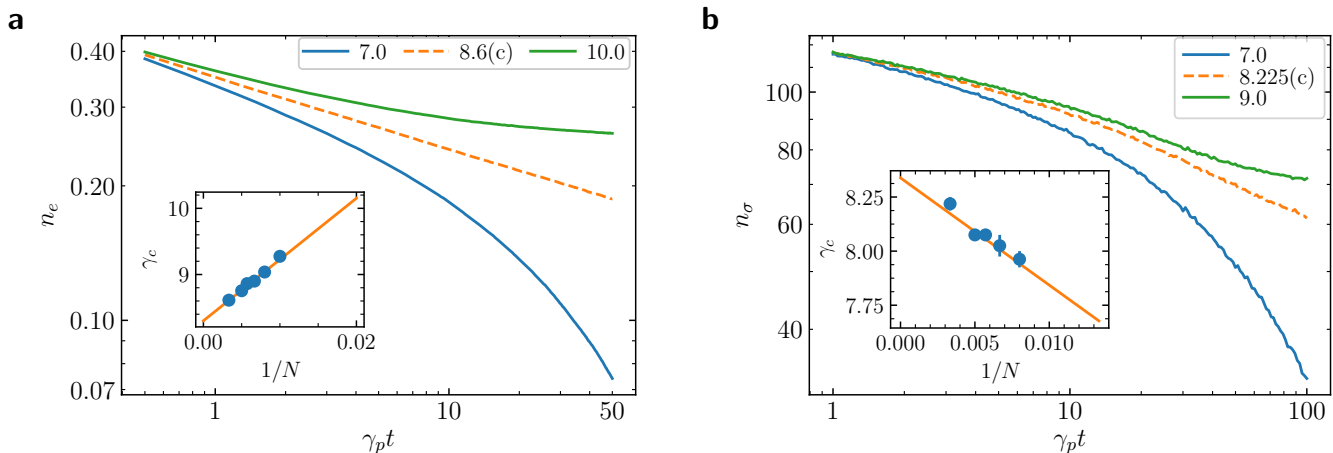


FIG. 2. Topological absorbing state transition. Error density n_e (a) and circuit depth n_σ (b) for $N = 300$ sites and different values of γ , showing subcritical behavior (blue), critical behavior (orange), and supercritical behavior (green). Initial states were chosen to have maximum n_e or n_σ , respectively. Finite size scaling leads to $\gamma_c = 8.30(2)$ (a, inset) and $\gamma_c = 8.34(5)$ (b, inset) in the thermodynamic limit.

by

$$c_i^h = \sqrt{\gamma} \sigma_i^x (1 - B_p) / 2, i \in p + 1,$$

with i being restricted to the upper rail. Essentially, the γ_p terms lead to a cooling dynamics removing errors with respect to the toric code ground state, while the γ terms describe a heating process introducing new errors. Importantly, the creation of a new error on the plaquette $p + 1$ requires the existence of another error on the neighboring plaquette p , which is also reflected after mapping onto Ising variables, see the Methods section for details. This results in the model falling into the well-known class of absorbing state models [35], with the toric code ground state corresponding to the absorbing state. Such absorbing state models can exhibit phase transitions to an active phase where the absorbing state is no longer reached asymptotically when starting from a different initial state. Here, we indeed find such a phase transition in the density of errors, see Fig. 2. Moreover, this absorbing-to-active transition is also accompanied by a divergence of the depth of the error correction circuit, i.e., by a topological transition to a trivial phase. We also track the critical exponent δ measuring the algebraic decay of the density of errors n_e or the circuit depth n_σ , respectively, by considering the quantity

$$\delta_{\text{eff}}(t) = -\frac{1}{\log m} \log \frac{n_{e,\sigma}(mt)}{n_{e,\sigma}(t)} \quad (2)$$

which remains constant for a fixed value of m [35]. In the limit of large system sizes, both the critical strength for the transition and the critical exponent are in close agreement between the absorbing-to-active transition and the topological transition, see Extended Data Fig. 4, belonging to the universality class of one-dimensional directed percolation ($\delta = 0.163$ [35]).

Importantly, our approach to topological order can also be readily applied to higher-dimensional systems. Here, we will be interested in a two-dimensional absorbing state model, in which both error types are present. In particular, the creation of A_v errors is conditional on the existence of a neighboring B_p error and vice versa. Hence, we consider jump operators of the form

$$c_i^{hv} = \sqrt{\gamma} \sigma_i^x (1 - A_v) / 2$$

$$c_i^{hp} = \sqrt{\gamma} \sigma_i^z (1 - B_p) / 2.$$

Importantly, the lack of boundary processes now leads to a conservation of the parity of both type of errors. This model can be expected to be in the same universality class as two-dimensional branching-annihilating random walks with two species [36]. While the model is active for any finite γ , it exhibits nontrivial critical behavior, having an exponent $\delta = 1$ with logarithmic corrections. Figure 3 shows the data collapse for different system sizes for both the error density and the circuit depth, confirming this picture. Strikingly, the logarithmic corrections in the topological case include a quadratic term that is not present in the error density, pointing to a different critical behavior. This demonstrates that topological criticality cannot be predicted using only the properties of an accompanying conventional phase transition.

In summary, we have introduced a novel operational approach to topological order based on the ability to perform topological error correction. Our method reproduces known topological phase transitions and can be readily applied to previously inaccessible cases such as topological transitions in open quantum systems, and has the additional advantage that it corresponds to a measurable observable. Finally, we would like to note that our approach can be readily applied to other topologically

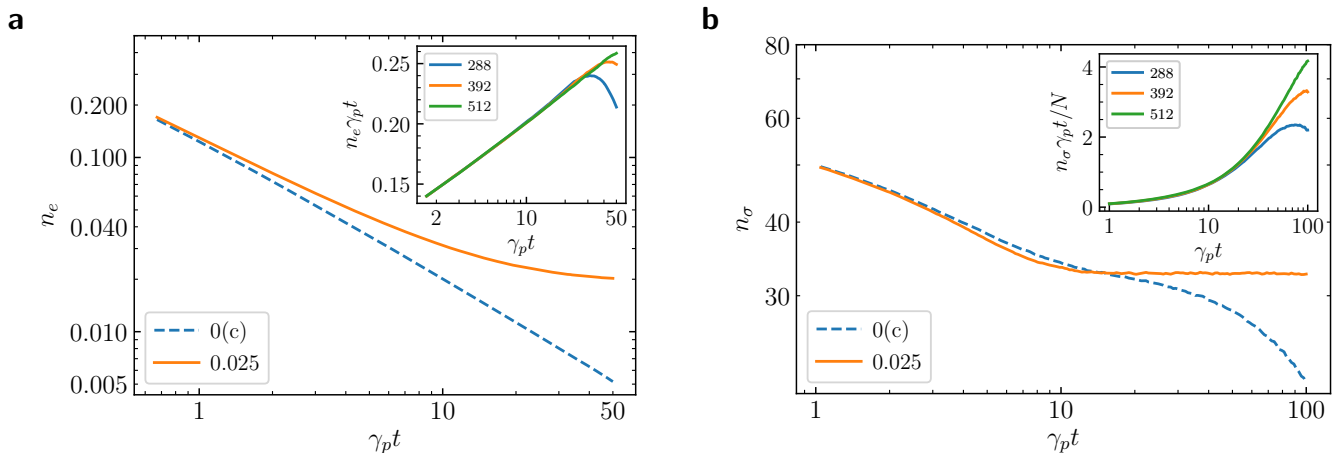


FIG. 3. Two-dimensional topological criticality. Error density n_e (a) and circuit depth n_σ (b) for $N = 512$ sites and $\gamma = 0$ (dashed) and $\gamma = 0.025 \gamma_p$ ($\gamma_p = \gamma_v$). The insets show the logarithmic corrections to a t^{-1} decay, with a linear behavior for the error density (a) and a quadratic behavior for the topological transition (b) before finite size effects become relevant.

ordered systems. For instance, both the Kitaev wire [37] and Haldane insulators [38] can be mapped onto effective spin models, where an analogous error correction strategy can be performed. Additionally, even exotic types such as fracton topological order [8, 9] can be expected to be classified in terms of their error correction properties [39].

METHODS

Error correction in toric code models

The error correction scheme for the detection of topological order is based on the results from the error syndrome measurements, which can be cast in terms of the spin variables S_v and S_p . In cases where there are both error types being present, the error correction can be realized independently. As the figure of merit, we are interested in the depth of the classical error correction circuit, which maps the initial erroneous state onto the topologically ordered state without any errors. Our error correction procedure is massively parallelized, i.e., within a topologically ordered phase, it is able to remove a thermodynamically large number of errors in constant time. This is in stark contrast to the conventional maximum-likelihood error correction [40], as this will always require an error correction circuit whose depth scales with the system size. The same argument also holds for assessing topological order based on circuit complexity [41], as the circuit complexity is an extensive quantity even in the topologically ordered phase.

For each error, we decorate the associated site with a walker w_i , which continuously explores the surroundings of the original site, looking for the presence of other

errors. In one spatial dimension, the walker alternates between investigating sites on the left and on the right, while in two dimensions, this is generalized to continuously exploring sites with an increasing Manhattan distance to the original site, see Extended Data Fig. 5. For simplicity, we assume that changing the site of a walker takes exactly one unit of time, irrespectively of the distance traveled. Once a walker encounters a site with either an error or a site previously visited by a walker w_j originating from another error, the error correction procedure starts. For this, the errors on site i and j are fused together along the shortest path, removing them and their associated walkers from the system. Here, we assume that the fusion is instantaneous, which does not modify the overall finite size scaling properties of the error correction circuit. The error correction procedure is performed until all errors have been removed from the system. In the one-dimensional case, we also allow for errors being removed via the left or right boundary of the system, preventing the case of a single error remaining without a potential fusion partner.

Ising-mapped jump operators

After mapping the system onto Ising variables S_i , we obtain a purely classical master equation, despite the basis states being highly entangled. Here, we take the limit $\gamma_v \rightarrow \infty$ such that the dynamics is restricted to the Ising spins related to the B_p operators. In the basis of the Ising spins S_i , we obtain the jump operators

$$c_i^p = \sqrt{\gamma_p} S_i^x S_{i+1}^x (1 - S_i^z) / 2$$

$$c_i^h = \sqrt{\gamma} S_{i+1}^x (1 - S_i^z) / 2.$$

DATA AVAILABILITY

The data that support the plots within this paper and other findings of this study are available from the corresponding author upon reasonable request.

ACKNOWLEDGMENTS

We thank S. Diehl and T. Osborne for fruitful discussions. This work was funded by the Volkswagen Foundation, by the Deutsche Forschungsgemeinschaft (DFG, German Research Foundation) within SFB 1227 (DQ-mat, project A04), SPP 1929 (GiRyd), and under Germanys Excellence Strategy – EXC-2123 QuantumFrontiers – 390837967.

AUTHOR CONTRIBUTIONS

Both authors contributed extensively to all parts of the manuscript.

COMPETING INTERESTS

The authors declare no competing interests.

* amit.jamadagni@itp.uni-hannover.de

- [1] Kitaev, A. Y. Fault-tolerant quantum computation by anyons. *Ann. Phys. (N. Y.)* **303**, 2–30 (2003).
- [2] Klitzing, K. v., Dorda, G. & Pepper, M. New Method for High-Accuracy Determination of the Fine-Structure Constant Based on Quantized Hall Resistance. *Phys. Rev. Lett.* **45**, 494–497 (1980).
- [3] Thouless, D. J., Kohmoto, M., Nightingale, M. P. & den Nijs, M. Quantized Hall Conductance in a Two-Dimensional Periodic Potential. *Phys. Rev. Lett.* **49**, 405–408 (1982).
- [4] Kohmoto, M. Topological invariant and the quantization of the Hall conductance. *Ann. Phys. (N. Y.)* **160**, 343 – 354 (1985).
- [5] Kitaev, A. & Preskill, J. Topological Entanglement Entropy. *Phys. Rev. Lett.* **96**, 110404 (2006).
- [6] Levin, M. & Wen, X.-G. Detecting Topological Order in a Ground State Wave Function. *Phys. Rev. Lett.* **96**, 110405 (2006).
- [7] Jiang, H.-C., Wang, Z. & Balents, L. Identifying topological order by entanglement entropy. *Nature Phys.* **8**, 902–905 (2012).
- [8] Chamon, C. Quantum Glassiness in Strongly Correlated Clean Systems: An Example of Topological Overprotection. *Phys. Rev. Lett.* **94**, 040402 (2005).
- [9] Haah, J. Local stabilizer codes in three dimensions without string logical operators. *Phys. Rev. A* **83**, 042330 (2011).
- [10] Kitagawa, T., Berg, E., Rudner, M. & Demler, E. Topological characterization of periodically driven quantum systems. *Phys. Rev. B* **82**, 235114 (2010).
- [11] Lindner, N. H., Refael, G. & Galitski, V. Floquet topological insulator in semiconductor quantum wells. *Nature Phys.* **7**, 490–495 (2011).
- [12] Wen, X.-G. Colloquium: Zoo of quantum-topological phases of matter. *Rev. Mod. Phys.* **89**, 041004 (2017).
- [13] Fidkowski, L. & Kitaev, A. Effects of interactions on the topological classification of free fermion systems. *Phys. Rev. B* **81**, 134509 (2010).
- [14] den Nijs, M. & Rommelse, K. Preroughening transitions in crystal surfaces and valence-bond phases in quantum spin chains. *Phys. Rev. B* **40**, 4709–4734 (1989).
- [15] Haegeman, J., Pérez-García, D., Cirac, I. & Schuch, N. Order Parameter for Symmetry-Protected Phases in One Dimension. *Phys. Rev. Lett.* **109**, 050402 (2012).
- [16] Pollmann, F. & Turner, A. M. Detection of symmetry-protected topological phases in one dimension. *Phys. Rev. B* **86**, 125441 (2012).
- [17] Elben, A. *et al.* Many-body topological invariants from randomized measurements in synthetic quantum matter. *Science Adv.* **6** (2020).
- [18] Dalla Torre, E. G., Berg, E. & Altman, E. Hidden Order in 1D Bose Insulators. *Phys. Rev. Lett.* **97**, 260401 (2006).
- [19] Chen, X., Gu, Z.-C. & Wen, X.-G. Local unitary transformation, long-range quantum entanglement, wave function renormalization, and topological order. *Phys. Rev. B* **82**, 155138 (2010).
- [20] Mora, C. E., Briegel, H. J. & Kraus, B. Quantum Kolmogorov complexity and its applications. *Int. J. Quant. Inf.* **05**, 729–750 (2007).
- [21] Zhang, Y., Grover, T., Turner, A., Oshikawa, M. & Vishwanath, A. Quasiparticle statistics and braiding from ground-state entanglement. *Phys. Rev. B* **85**, 235151 (2012).
- [22] Zhu, W., Sheng, D. N. & Haldane, F. D. M. Minimal entangled states and modular matrix for fractional quantum Hall effect in topological flat bands. *Phys. Rev. B* **88**, 035122 (2013).
- [23] Bridgeman, J. C., Flammia, S. T. & Poulin, D. Detecting topological order with ribbon operators. *Phys. Rev. B* **94**, 205123 (2016).
- [24] Jamadagni, A., Weimer, H. & Bhattacharyya, A. Robustness of topological order in the toric code with open boundaries. *Phys. Rev. B* **98**, 235147 (2018).
- [25] Terhal, B. M. Quantum error correction for quantum memories. *Rev. Mod. Phys.* **87**, 307–346 (2015).
- [26] Tagliacozzo, L. & Vidal, G. Entanglement renormalization and gauge symmetry. *Phys. Rev. B* **83**, 115127 (2011).
- [27] Trebst, S., Werner, P., Troyer, M., Shtengel, K. & Nayak, C. Breakdown of a Topological Phase: Quantum Phase Transition in a Loop Gas Model with Tension. *Phys. Rev. Lett.* **98**, 070602 (2007).
- [28] Wootton, J. A Simple Decoder for Topological Codes. *Entropy* **17**, 1946–1957 (2015).
- [29] Hastings, M. B. Topological Order at Nonzero Temperature. *Physical Review Letters* **107** (2011).
- [30] Bardyn, C.-E. *et al.* Topology by dissipation. *New J. Phys.* **15**, 085001 (2013).
- [31] Viyuela, O., Rivas, A. & Martin-Delgado, M. A. Two-Dimensional Density-Matrix Topological Fermionic

- Phases: Topological Uhlmann Numbers. *Phys. Rev. Lett.* **113**, 076408 (2014).
- [32] Huang, Z. & Arovas, D. P. Topological Indices for Open and Thermal Systems Via Uhlmann’s Phase. *Phys. Rev. Lett.* **113**, 076407 (2014).
- [33] Grusdt, F. Topological order of mixed states in correlated quantum many-body systems. *Phys. Rev. B* **95**, 075106 (2017).
- [34] Weimer, H., Müller, M., Lesanovsky, I., Zoller, P. & Büchler, H. P. A Rydberg quantum simulator. *Nature Phys.* **6**, 382–388 (2010).
- [35] Hinrichsen, H. Non-equilibrium critical phenomena and phase transitions into absorbing states. *Adv. Phys.* **49**, 815–958 (2000).
- [36] Ódor, G. Critical branching-annihilating random walk of two species. *Phys. Rev. E* **63**, 021113 (2001).
- [37] Kitaev, A. Y. Unpaired Majorana fermions in quantum wires. *Phys.-Usp.* **44**, 131 (2001).
- [38] Haldane, F. D. M. Nonlinear Field Theory of Large-Spin Heisenberg Antiferromagnets: Semiclassically Quantized Solitons of the One-Dimensional Easy-Axis Néel State. *Phys. Rev. Lett.* **50**, 1153–1156 (1983).
- [39] Qiu, Y. & Wang, Z. Ground Subspaces of Topological Phases of Matter as Error Correcting Codes. *arXiv:2004.11982* (2020).
- [40] Dennis, E., Kitaev, A., Landahl, A. & Preskill, J. Topological quantum memory. *J. Math. Phys.* **43**, 4452–4505 (2002).
- [41] Liu, F. *et al.* Circuit complexity across a topological phase transition. *Phys. Rev. Research* **2**, 013323 (2020).

Extended data

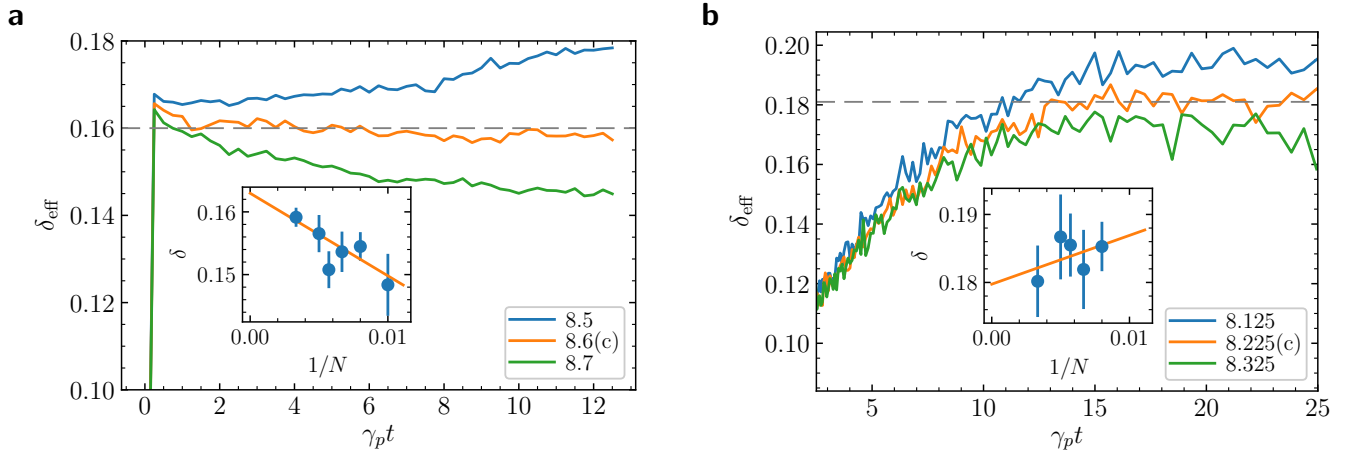


FIG. 4. Effective critical exponents according to Eq. (2) for the absorbing-active transition (a) and the topological transition (b) ($m = 4$). The critical value of the transition is taken where δ_{eff} remains constant. Error bars correspond to all values consistent with a constant value in the long time limit. Finite size scaling leads to $\delta = 0.163(5)$ (a, inset) and $\delta = 0.18(2)$ (b, inset) in the thermodynamic limit. Errors are given by the sum of the uncertainty in the linear fit and the difference in δ between $m = 4$ and $m = 2$.

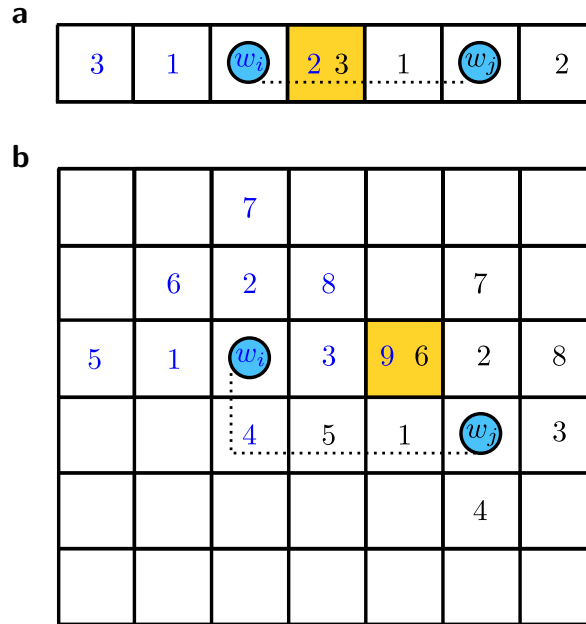


FIG. 5. Schematic representation of the error correction procedure. Two errors are associated with walkers w_i (blue) and w_j (black), located at the errors at $t = 0$. The colored numbers indicate the timestep at which a particular walker visits a site. Once a walker encounters a site already visited by the other walker (yellow), the two errors can be fused along the dotted path. In one dimension (a), the walkers alternate in a left-right pattern, in two dimensions (b), the walkers proceed in diamond-shaped patterns corresponding to a constant Manhattan distance from the initial sites.